Influence of Solid Particles on Cavitation in Poly(methylene oxide) during Crystallization

Radoslaw Nowacki, Ewa Piorkowska

Centre of Molecular and Macromolecular Studies, Polish Academy of Sciences, 90 363 Lodz, Poland

Received 2 November 2006; accepted 18 January 2007
DOI 10.1002/app.26186
Published online 9 April 2007 in Wiley InterScience (www.interscience.wiley.com).

ABSTRACT: Cavitation in pockets of melt occluded by impinging spherulites during isothermal crystallization of poly(methylene oxide) was explored. A reason for cavitation is a negative pressure buildup in pockets because of the change of density during crystallization. Compositions of poly(methylene oxide) with talc and chalks unmodified and modified with calcium stearate were studied to determine the influence of foreign solid particles on the cavitation. The crystallization and cavitation in polymer films were observed by a light microscopy; sample surfaces were examined also under SEM. The spherulite growth rate, decreasing under negative pressure, was measured and used to estimate the negative pressure level at the moment of cavitation that is the strength of the polymer melt. Chalk modified with calcium stearate drastically lowered the strength of poly(methylene oxide) melt, whereas unmodified chalk did not. The effect depended on the chalk content and on the particle size. The results demonstrate that the cavitation in a polymer melt under the negative pressure is nucleated by solid particles poorly adhering to a polymer. © 2007 Wiley Periodicals, Inc. J Appl Polym Sci 105: 1053–1062, 2007

Key words: crystallization; cavitation; negative pressure

INTRODUCTION

Cavitation, the process of rupturing a liquid by a decrease in pressure at a roughly constant temperature, was intensively studied in low molecular weight liquids, especially in water, during the last century.[1] In a pure liquid, having the surface tension, σ; the pressure, p; exterior to a bubble of radius, R; is related to the interior pressure, p_B.

$$p_B - p = \triangle p = 2\sigma/R \quad (1)$$

To maintain the equilibrium, the exterior liquid pressure, p, has to be less than p_B. If p is maintained at a constant value just slightly less than $p_B - 2\sigma/R$, the bubble will grow, and rupture will occur. The value of $\Delta p_c = p_B - p_c$, corresponding to the pressure p_c, at which the cavitation occurs is called the tensile strength of a liquid. To avoid confusion with tensile drawing we will call it here simply ''strength.'' We note that if $p_B > p_c$, which is always fulfilled when cavitation occurs at the negative pressure, the strength Δp_c has a positive value.

In the theory of homogeneous nucleation of cavitation[2,3] the energy barrier of the formation of cavitation nucleus, W, consists of the positive component associated with the formation of a bubble surface and the negative component, because describing the work necessary to empty the volume of a bubble and replace it with saturated vapor of liquid. The energy W passes through a maximum for a critical value of the radius: $R_c = 2\sigma/\Delta p$. Zheng et al.[4] found that the extreme negative pressure that caused the cavitation in aqueous microinclusions in minerals at 43°C was −140 MPa, close to the range from −130 to −140 MPa that was predicted based on the theory of homogeneous nucleation, although water in larger portions exhibits usually much lower strength, for instance: 5 MPa,[5] 19 MPa,[6] 27.7 MPa.[7] The experimentally determined low strength and, at the same time, a scatter of data are attributed to heterogeneous nucleation of the cavitation; the most efficient nuclei in water are supposed to be hydrophobic solid particles with crevices filled with residue of air.[8]

Much less is known about the cavitation during crystallization. The cavitation was observed during crystallization in a number of substances subjected to negative pressure, for instance: capric acid, paraffin, and potassium sulfite; however not during their melting.[9] Recently, the cavitation was observed during crystallization of ice in an ultrasonic field; bubbles were generated preferably at the solid–liquid interface.[10]

In polymers, in pockets of melt occluded by impinging spherulites, the crystallization is accompanied by a buildup of negative pressure because of a

Correspondence to: E. Piorkowska (epiorkow@bilbo.cbmm.lodz.pl).

Contract grant sponsor: State Committee for Scientific Research, Poland; contract grant numbers: 4 T08E 055 22, 4T08E 095 25.

lower specific volume of solidified material.[11–17] The negative pressure can grow to a certain limit, beyond which the cavitation occurs and the melt fractures. However, the whole pocket can solidify under negative pressure, without any visible cavitation. Local stresses and holes developed in the occluded pockets of melt weaken the material; hence, those places constitute ''weak spots'' of the spherulitic structure.

Computer simulation of spherulitic crystallization, confirmed experimentally, indicated that in a uniform temperature field the weak spots occupy up to about 13% of a film surface and up to 0.5 vol % of a polymer in bulk, respectively.[11,17] When crystallization of a polymer bulk originates from outer surfaces e.g., because of cooling and/or surface nucleation, the entire volume deficiency cumulates in the polymer interior and the weak spots occupy a significant fraction of a crystallizing material.

The negative pressure lowers the equilibrium melting temperature, T_m°, hence it decreases the undercooling, which is reflected in a decrease in the growth rate of spherulites and in an increase of lamellae thickness within weak spots.[12,13] The cavitation, when occurs, relaxes the negative pressure in the melt and the growth rate abruptly increases to its initial value, characteristic of atmospheric pressure at a given temperature.[12,15] A sudden pressure change associated with cavitation caused an acoustic emission during crystallization which was evidenced for isotactic polypropylene (iPP) and poly(methylene oxide) (POM).[16] Glow discharge induced by a high-frequency electric field in freshly formed cavitation bubbles in iPP indicated that the pressure inside was far below atmospheric pressure.[11] Nucleation of new iPP spherulites, frequently of the β crystallographic form, on outer surfaces of the cavitation bubbles was also reported.[15,18]

Holes formed in crystallizable polymers during their solidification upon processing undoubtedly lower their mechanical performance. Better understanding of the cavitation phenomena during crystallization is then of great importance. The cavitation in the amorphous interlamellar layers was recently found to play a vital role in plastic deformation of semicrystalline polymers during tensile drawing[19,20]; knowledge of the level of negative pressure that causes cavitation during crystallization was useful in understanding the deformation process.

Although a number of facts concerning the cavitation during polymer crystallization are known, the systematic studies of this phenomenon were conducted so far only for one grade of iPP.[15] Only preliminary observations were conducted for another polymer, POM.[21] In Ref. 15 the evaluation of negative pressure value in weak spots was based on the depression of spherulite growth rate caused by the shift of the equilibrium melting temperature under pressure. According to the Lauritzen–Hoffman theory, at the temperature, T, well above the glass transition of polymer, the spherulite growth rate is controlled by the factor $\exp\left[-K_g/T\ (T_m^\circ - T)\right]$, where K_g is a constant characteristic of a given polymer and of the crystallization regime. The shift of equilibrium melting temperature, ΔT_m°, can be then calculated, based on the spherulite growth rate change:

$$\triangle T_m^o = T_m^o - T - \left\{ (T_m^o - T)^{-1} + T\ K_g^{-1} \ln\left(\frac{G}{G_p}\right) \right\}^{-1} \tag{2}$$

where G and G_p denote the growth rates under atmospheric pressure, p_{atm}, and under negative pressure, p, respectively. Since polymers do not evaporate, and the pressure of gas inside a bubble is negligibly small, the strength of a polymer melt equals:

$$\triangle p = -\left[p_{\mathrm{atm}} - \triangle T_m^o / \left(dT_m^o/dp\right)\right] \tag{3}$$

where dT_m°/dp can be extrapolated for a given polymer from a positive pressure range. Equation (3) requires linear $T_m^\circ\ (p)$ dependence that is probably true when the pressure is not extremely negative.

The strength of iPP melt determined based on the growth rate measurements and using eqs. (2) and (3) varied very significantly in different weak spots during crystallization at the same temperature.[15] The scatter of cavitation threshold, suggestive of predominant influence of impurities, is contradictory to the observation that cavitation bubbles were always formed in iPP at the spherulite-melt interphase, that seems to indicate a decisive role of solid–liquid interface in the cavitation phenomena. The cavitation in weak spots occurred only below a certain limiting temperature, whereas at a higher crystallization temperature the cavitation along interspherulitic boundaries was observed instead.[15,22,23]

In the present article we undertook systematic studies of cavitation during crystallization of POM to find out if phenomena observed in iPP[15] are typical of other polymers. Large cavities are frequently found in extruded or injection molded shapes of POM [e.g.[24]] that indicates the importance of the studies of cavitation phenomena in this polymer, whose high crystallinity level and high volume change during crystallization facilitate negative pressure buildup and cavitation.

To shed more light on the void formation mechanism we have explored the cavitation not only in neat POM but also in talc nucleated POM, and also in POM with a chalk filler. The cavitation during crystallization in a polymer with solid particles

introduced on purpose was not studied so far, although, the effect of solid particles on cavitation in water is well known.[1] To vary the adhesion between chalk particles and POM melt, unmodified chalk particles of calcite crystallographic form and a calcium stearate modified chalk particles were utilized.

The cavitation in polymer films between two glass slides was studied during isothermal crystallization at different temperatures by light microscopy. The spherulite growth rate in the occluded pockets of melt was measured. Negative pressure in those pockets and strength of the polymer melts were estimated based on eqs. (2) and (3).

EXPERIMENTAL

Materials and sample preparation

Polyacetal (POM) type of a polymer, Tarnoform 300 Natural, produced by Zaklady Azotowe SA, Tarnow, Poland, by copolymerization of trioxane with $\sim$ 2–3 wt % of 1,3 dioxolane, having MFI = 9 $\pm$ 1 g/10 min (2.16 kg, 190°C) was used in the study.

Talc used as a nucleating agent for POM, Steamic S, purchased from Luzenac, France, had the weight average particle size of 1.8 μm. This mineral will be referred to as talc although it contains on average 79% of talc, 20% of chlorite, and 1% of dolomite.

Three types of chalk were utilized as fillers: Setacarb OG (C1), ground unmodified chalk with weight average particle size of 0.440 μm, purchased from Omya, Switzerland, and two types of precipitated, calcium stearate modified chalks, SuperPflex 200 (C2) and Winnofil SPT (C3) obtained from Specialty Minerals, USA and ICI, United Kingdom, respectively. The weight average particle size and modifier content were: 0.700 μm and 2 wt % for C2 and 0.075 μm and 2.4 wt % for C3.

Compositions of POM with 1 and 5 wt % of chalks were obtained by melt blending in a Brabender mixer (Brabender OHG, Germany) at 185°C for 10 min, at 60 rpm under a flow of nitrogen. Neat POM was also processed in the same way for comparison.

Thirty-micrometer-thick films sandwiched between two microscope cover slides were prepared for light microscopy by compression molding at 190°C. Uniform thickness was ensured by ring shaped aluminum foil spacers placed at the edges of glasses. Film thickness of the talc nucleated POM was reduced to 15 μm to increase the average size of spherulites and the size of pockets of melt.

Methods

The crystallization and cavitation in polymer films was studied in a Linkam hot stage THMS600 equipped with a temperature control unit TMS92 (Linkam Scientific Instruments, United Kingdom). The hot stage was mounted on a polarized light microscope connected to a CCD camera, CRT display, VHS video recorder and a computer equipped with a frame grabber card, which permitted to monitor samples during the entire thermal treatment. Time was measured using a Linkam Video Text Overlay VTO 232 with the precision of 0.1 s. Images were recorded at the rate of 1 per 0.04 s.

The films were melt annealed for 3 min at 190°C and then cooled at 10 K/min to a desired crystallization temperature chosen from the range of 151–161°C. After crystallization, the samples were cooled at 5 K/min to room temperature. The entire procedure was conducted under a flow of dry gaseous nitrogen to prevent polymer degradation. Several samples, at least three, of each material and for each crystallization conditions were crystallized and studied. Microscope glasses produced by Chance Proper, United Kingdom, and Menzel-Glaser, Germany, were utilized in the study after washing in ethanol. No difference in the cavitation phenomena because of the use of glass slides supplied by different producers was observed. Scratches on the glasses, also made on purpose, did not influence markedly the cavitation process.

Spherulite growth rate, G, for all materials studied was calculated from the changes of crystallizing front positions in successive time intervals. G was measured also within weak spots to determine the negative pressure buildup, especially at the moment of cavitation; care was taken to determine G in short time intervals just before cavitation. The G values measured for isolated spherulites were used to construct a temperature dependence of the growth rate and to calculate K_g parameters, used in eq. (2). Progression of crystallization in weak spots, beginning with the moment of occlusion of melt pockets by spherulites, was also followed by light microscopy.

Upper glasses were removed from the samples after postcrystallization cooling. The specimens were sputtered with gold and examined under a Jeol 5500LV scanning electron microscope.

TA Instrument DSC 2920, was applied to determine the dependence of crystallinity level on crystallization temperature. Specimens having the mass of 7–8 mg were heated up to 190°C, melt annealed at 190°C for 3 min and then cooled at 10 K/min to a crystallization temperature. After the isothermal crystallization, they were cooled to room temperature and heated up again at 10 K/min, to determine the melting enthalpy.

RESULTS AND DISCUSSION

Figure 1 shows a typical sequence of phenomena observed during spherulitic crystallization in the

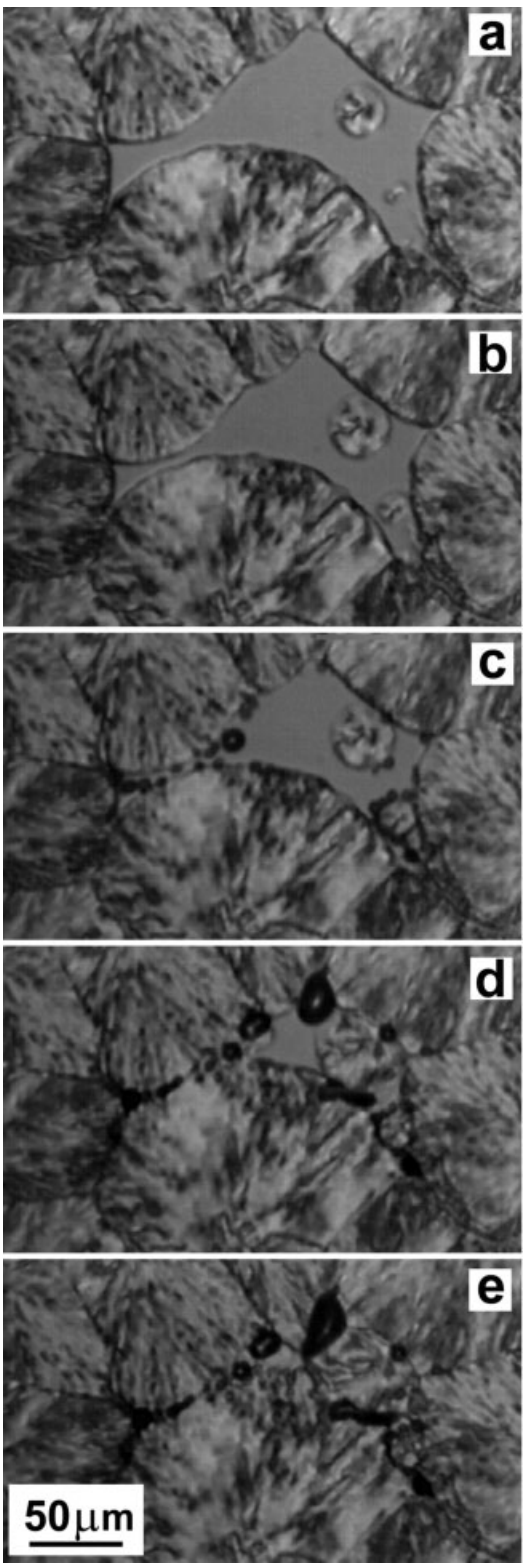

Figure 1 Polarized light micrographs showing consecutive stages of crystallization and cavitation in a weak spot in POM film at 154°C: (a) occlusion of the melt by spherulites, (b) crystallization before cavitation, (c) cavitation (cavities are visible as black circles) (d) postcavitation crystallization, (e) final structure.

thin films of neat POM between microscopic glasses. The impinging spherulites blocked the influx of the melt into the melt pocket—the weak spot. Accumulation of volume deficiency resulted in the negative pressure buildup. When it reached a sufficient level, the cavitation occurred that released abruptly the negative pressure. Bubbles of different sizes were always formed inside observed weak spot simultaneously, that is within the 0.04 s interval of a single frame recording. They appeared predominantly at the interface of melt—crystallizing front, often in the vicinity of interspherulitic boundaries. The bubbles inside the melt, away from a growth front of spherulite were seen much less frequently. After the cavitation, the bubbles either became occluded by growing spherulites or were expanding until the end of crystallization in a weak spot. Some of the bubbles caused nucleation of new spherulites as it was demonstrated in Ref. 21. A bubble collapse was observed very rarely. These features of the cavitation process are very similar to those observed for iPP.[15,21] Possible reasons of spherulite nucleation on the cavitation bubbles were already discussed in Refs. 15, 18.

During crystallization of POM at 156–157°C the cavitation was seldom and practically ceased above 157°C; only one cavitation event was recorded for several samples at 159°C.

SEM studies of surfaces of the isothermally crystallized films of POM, shown in Figure 2 revealed voids of different sizes visible within the weak spots. Chains of small cavities found in iPP at the crystallizing fronts in the vicinity of glasses confining a polymer film[15] were observed in POM much less frequently.

The cavitation along interspherulitic boundaries, reported in Ref. 15 for iPP, was marginal in POM either during isothermal crystallization or during postcrystallization cooling. Previously[15,21] we concluded

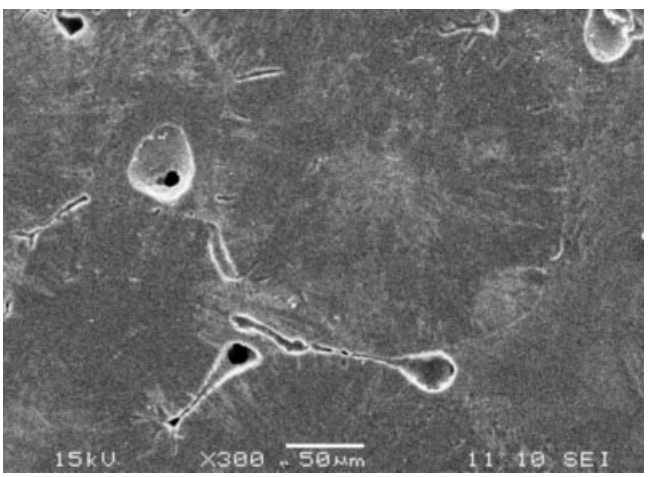

Figure 2 SEM micrograph of surface of POM film crystallized at 154°C.

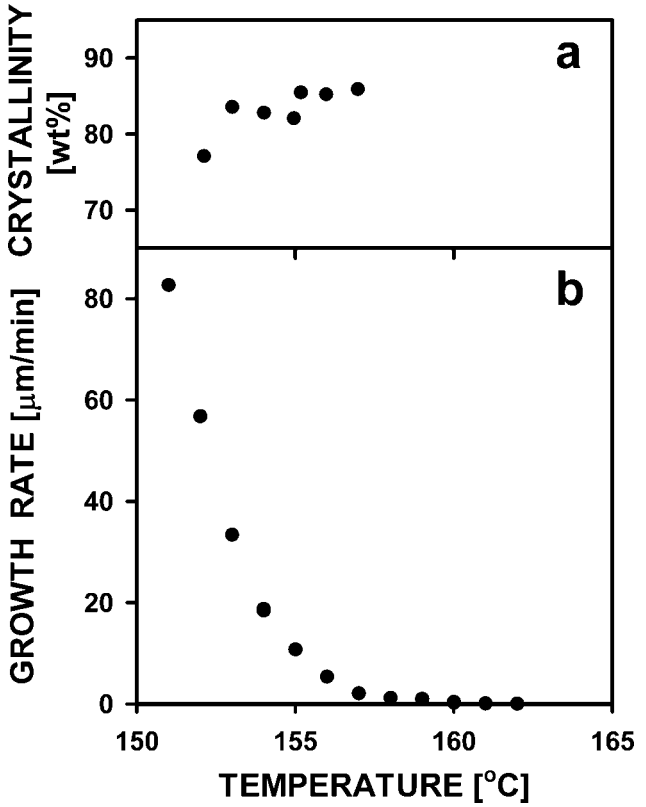

Figure 3 Temperature dependencies of crystallinity level (a) and spherulite growth rate (b) for POM.

that the bubble formation along interspherulitic boundaries was related to fractionation during crystallization, reflected also in a decrease of the spherulite growth rate with time. The growth rate stability in time is an indication of low level of fractionation during crystallization. In POM the spherulite growth was stable during crystallization, which also corresponded to the low level of cavitation along the interspherulitic boundaries.

The temperature dependencies of the spherulite growth rate and the crystallinity level of POM studied, are plotted in Figure 3. To calculate the crystallinity level the melting enthalpy of POM crystals equal to 221.9 J/g[25] was assumed. K_g constant, required to estimate negative pressure according to eqs. (2) and (3), was determined based on the plot of $\ln G + Q_D/RT$ against $1/T\Delta T$. The value of 7 kcal/mol as the activation energy of reptation, Q_D, and T_m° of 198.3°C[26] were used for this purpose. In the temperature range 151–159°C the plot was linear; the calculated value of K_g was equal to 6.1×10^5 K^2 and close to that determined in Ref. 26 A shift in T_m° and a negative pressure in POM weak spots were calculated according to eqs. (2) and (3) and assuming $dT_m^\circ/dp = 0.156$ K/MPa.[27]

In all weak spots studied the spherulite growth rate decreased from the moment of occlusion, as it is illustrated in Figure 4. Cavitation released the negative pressure that caused an abrupt increase of the growth rate to its initial value, typical of atmospheric pressure. In Figure 5(a) the spherulite growth rate scaled to its initial value is plotted against the conversion degree of the melt into spherulites in weak spots of various initial surface areas. The conversion degree in weak spots was measured from the moment of melt occlusion by spherulites. In Figure 5(b) the respective shift in T_m° and the corresponding negative pressure are plotted as functions of the conversion degree. A decrease of the growth rate, hence the negative pressure buildup, depended on the initial size of a weak spot. In larger weak spots the decrease of the growth rate with the increase of the conversion degree was faster and the cavitation occurred earlier. The increase of crystallization temperature to 156°C resulted in a slower deceleration of the growth rate and the cavitation did not occur in the observed weak spots unlike in those at 154°C. Figure 6 demonstrates that during POM crystallization at 155°C the cavitation occurred in smaller weak spots at later stages of conversion of melt into spherulites whereas in the smallest weak spots the cavitation was not observed at all.

The negative pressure originates from volume deficiency, thus the decrease of the spherulite growth rate should depend solely on the conversion level in a weak spot, especially as the crystallinity level of POM determined by DSC measurements is stable in the temperature range of 153–157°C. The above relations invoke a slower buildup of the negative pressure in smaller weak spots and at higher crystallization temperature.

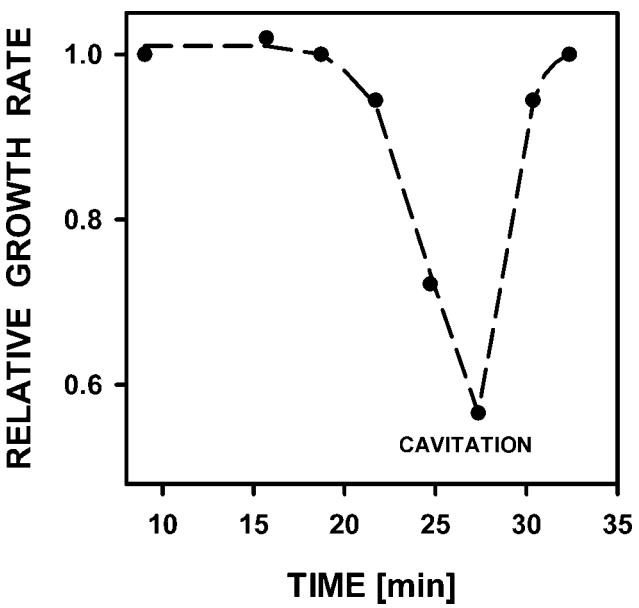

Figure 4 Spherulite relative growth rate versus time in a weak spot in POM during crystallization at 157°C.

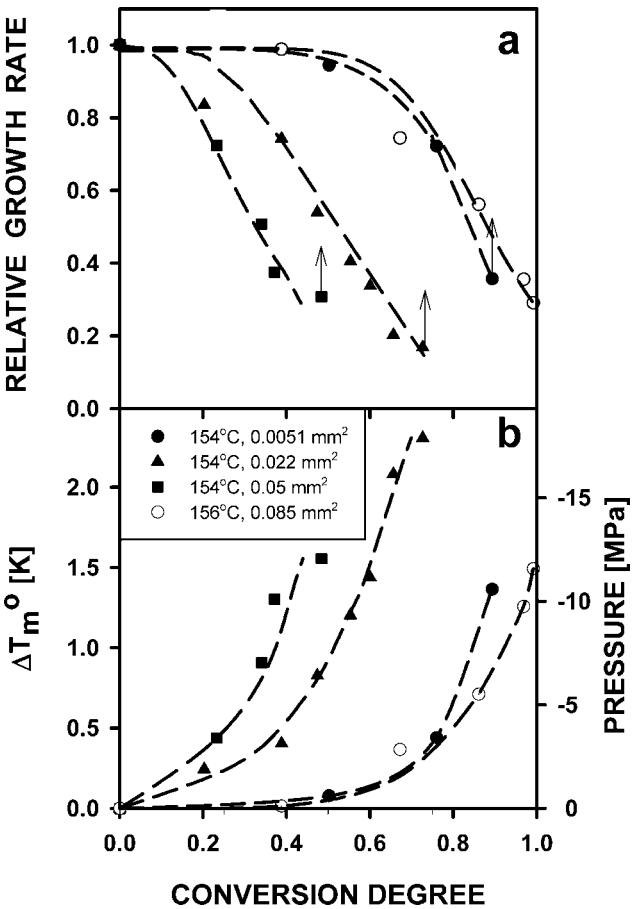

Figure 5 Spherulite relative growth rate (a), shift in T_m° and corresponding negative pressure (b) both versus conversion degree in weak spots of different initial size in POM film during crystallization at 154 and 156°C. Crystallization temperature and initial surface area of each weak spot in the legend. Arrows indicate cavitation.

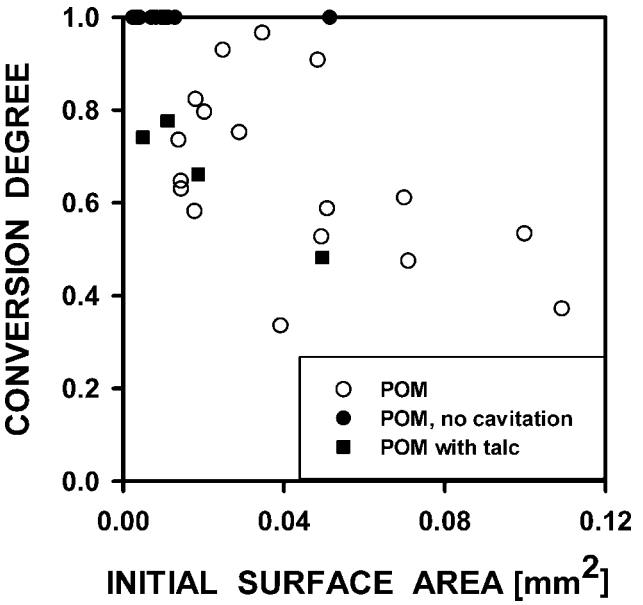

Figure 6 Conversion degree at the moment of cavitation plotted against a weak spot initial surface area during crystallization of POM and POM with talc at 155°C. Initial surface area of small weak spots in POM in which the cavitation was not observed denoted by filled circles.

The strength of POM melt in weak spots and the corresponding shift in T_m°, according to eqs. (2) and (3), are plotted as functions of crystallization temperature in Figure 7. The highest melt strength is about 18 MPa. The data are scattered, similarly as it was previously found for iPP.[15] The average values reveal a tendency to decrease slightly with an increase of the crystallization temperature.

Examples of light micrographs of the cavitation in POM compositions with talc and chalks are shown in Figures 8 and 9 whereas respective SEM micrographs in Figure 10. A drop of T_m° at the moment of cavitation and the corresponding melt strength of POM with talc and chalks are plotted against crystallization temperature in Figure 11.

The cavitation in POM with talc was observed up to the crystallization temperature of 157°C, similarly as in neat POM. In POM with talc the cavitation phenomena were similar to those in neat POM, except for few differences. The cavitation bubbles in POM with talc appeared frequently within the polymer melt far from the spherulite-melt interface; in some weak spots the bubbles were formed exclusively away from the crystallization front, as shown in Figure 8. A complicated bubble shape, like that visible in Figure 8, was found also in other weak spots, most probably because of merging of few smaller voids located close to each other. However, the merging process was too fast to be resolved with the help of the recording equipment. Another differ-

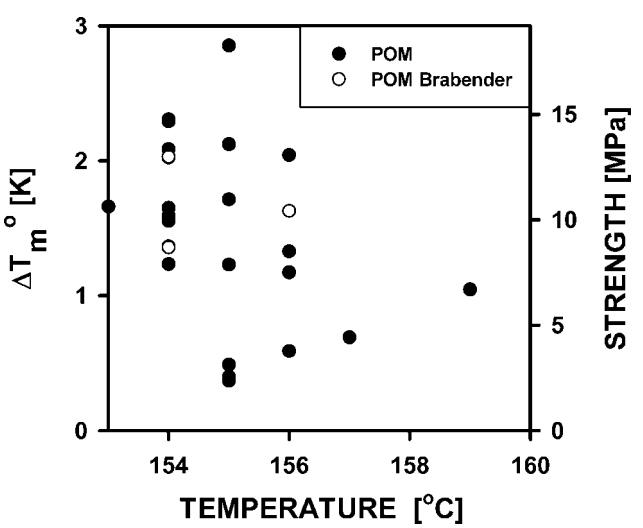

Figure 7 Shift in T_m° at the moment of cavitation and corresponding melt strength of POM versus crystallization temperature.

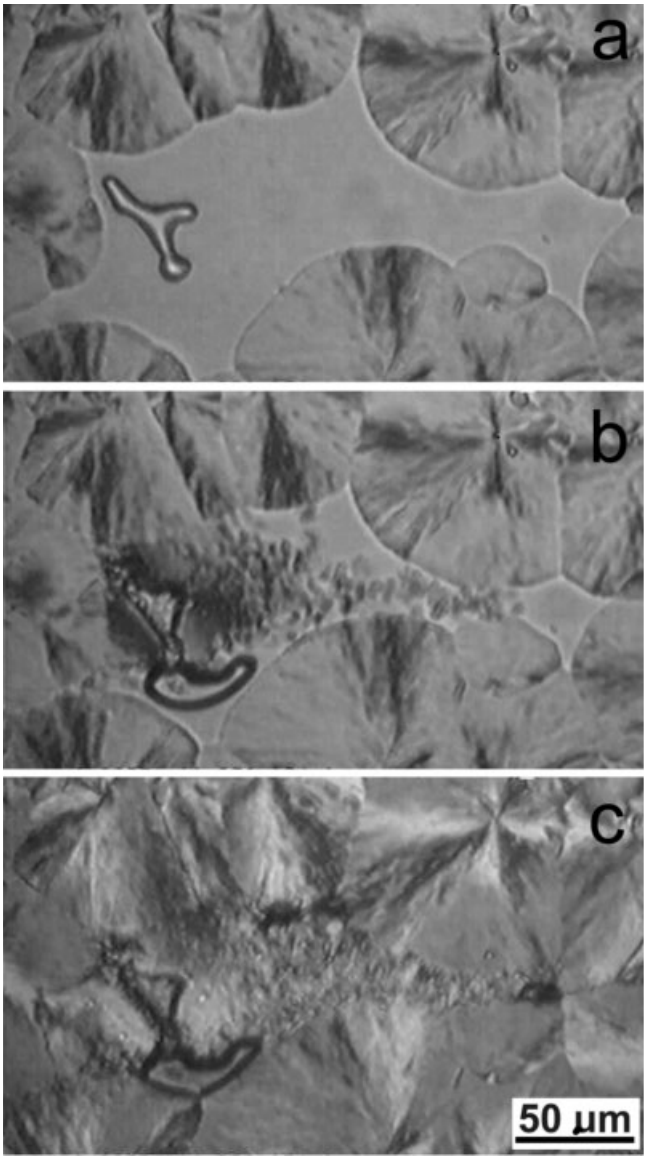

Figure 8 Sequence of polarized light micrographs showing cavitation, postcavitation crystallization, and final structure in a weak spot in POM with talc at 154°C.

ence between neat POM and talc nucleated POM was that in the latter after the cavitation numerous fine spherulites were nucleated and filled quickly the entire interior of a weak spot.

The dependence of the conversion degree at the moment of cavitation against the initial size of a weak spot in POM with talc during crystallization at 155°C plotted in Figure 6, reveals the same tendency as in neat POM. However, the cavitation in POM with talc occurred also in much smaller weak spots than in neat POM.

Data points indicating the drop of T_m° at the moment of cavitation and the corresponding melt strength of POM with talc, plotted in Figure 11(a), are scattered for each crystallization temperature, similarly as for neat POM. However, more data points assume lower ΔT_m° values for POM with talc than without talc.

Cavitation in POM with chalk was studied at 154, 156, and 158°C. That was because in neat POM an intense cavitation occurred at 154°C, less frequently at 156°C and it was absent at 158°C. The addition of unmodified chalk C1 to POM did not influence markedly the cavitation during crystallization. The only difference noticed was that the cavitation occurred also at 158°C in the samples with 5 wt % of C1 chalk; the bubbles appeared at the spherulite-melt interface. On the contrary, C2 chalk modified with calcium stearate influenced markedly the cavitation process as it is demonstrated in Figure 9. The cavitation occurred exclusively inside the polymer melt shortly after occlusion by spherulites and no bubble at the spherulite-melt interface was ever noticed. In the films with 5 wt % of C2 chalk in each weak spot only one single bubble appeared and grew larger. SEM micrographs in Figure 10 show large bubbles in POM with talc and in POM with 5 wt % of modified C2 chalk. Small particles visible inside the bubble in Figure 9(b) have the size corresponding to the sizes of chalk particles. For that

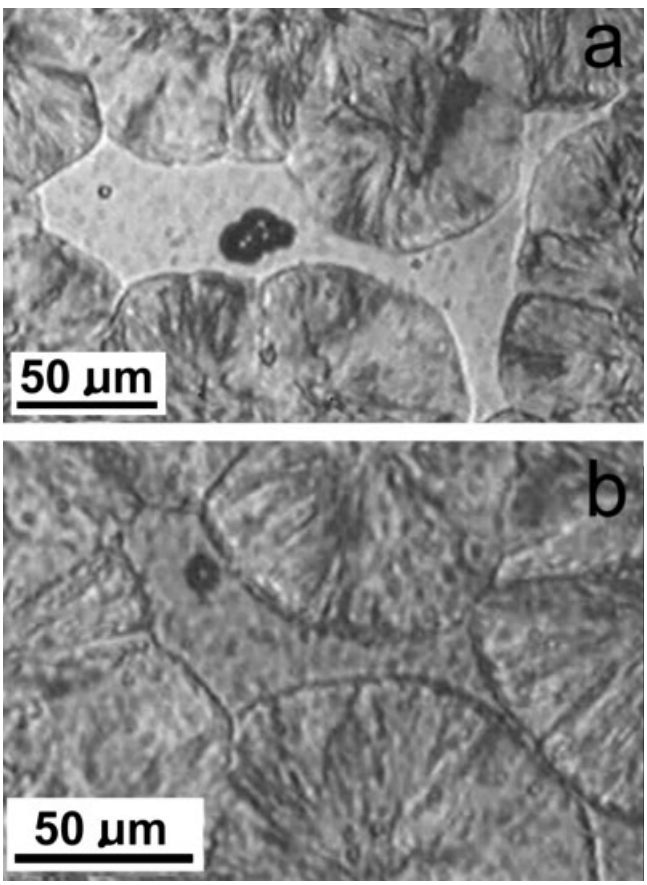

Figure 9 Polarized light micrograph of cavitation bubbles in weak spots in POM with C2 chalk during crystallization at 154°C: (a) 1 wt % of C2, (b) 5 wt % of C2.

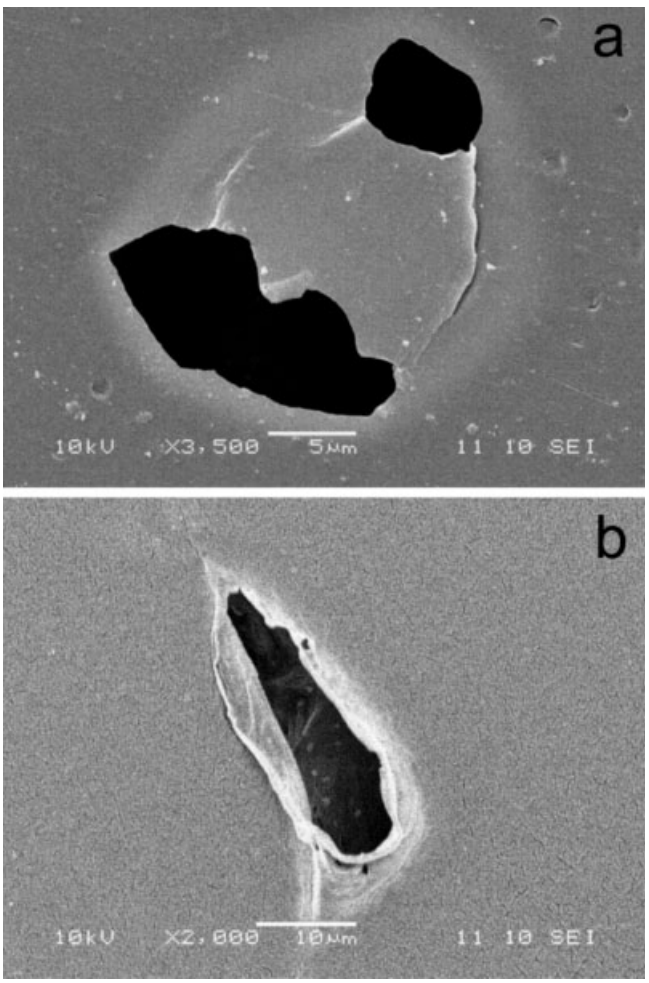

Figure 10 SEM micrographs of voids: (a) in POM with talc crystallized at 154°C, (b) in POM with 5 wt % of C2 chalk crystallized at 156°C.

composition the cavitation was also observed during crystallization at 158°C in each sample studied and it was still visible at 159°C. It must be mentioned here that no difference was detected between neat POM films obtained from pellets and from the polymer processed in the Brabender mixer in the same way as the compositions with chalk particles as shown in Figure 7.

C3 chalk, modified by calcium stearate but with particles smaller than those of C2 chalk influenced the cavitation phenomena only in a limited way. The cavitation occurred at the spherulite-melt interface and also within the polymer melt; single cavitation bubbles inside the polymer melt, far from spherulite-melt interface were sometimes observed. In POM with 5 wt % of C3 chalk the cavitation was detected also at 158°C.

The T_m° decrease at the moment of cavitation and the corresponding melt strength calculated based on the growth rate measurements according to eqs. (2) and (3) for the films of POM with chalks are collected in Figure 11. The unmodified chalk did not influence the strength of POM melt. The data were scattered for each crystallization temperature, similarly as for neat POM. The strength of POM melt with modified C2 chalk was much lower than that of neat POM, especially for the chalk content of 5 wt %. The cavitation occurred readily at the negative pressure of −0.6 MPa. C2 chalk reduced also the experimental data scatter. The melt strength of POM with 5 wt % of C2 chalk was nearly independent of temperature. The strength of POM melt with modified C3 chalk was intermediate between those of neat POM and POM with C2 chalk.

DISCUSSION AND CONCLUSIONS

The cavitation in neat POM during crystallization, depending on the crystallization temperature, revealed similarities to that in iPP studied previously.[15]

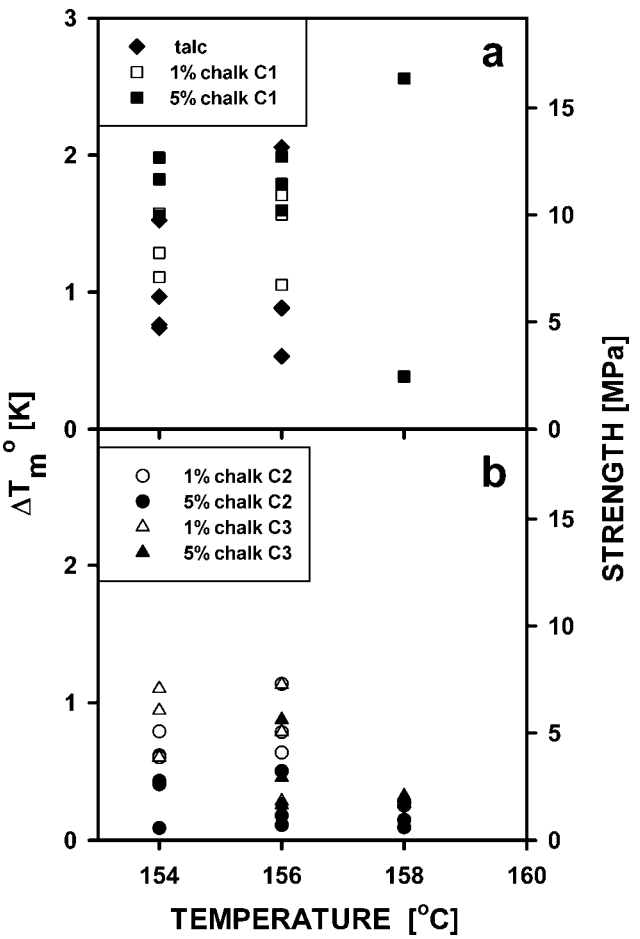

Figure 11 Shift in T_m° at the moment of cavitation and corresponding melt strength of POM with talc and chalks versus crystallization temperature: (a) POM with talc and POM with C1 chalk, (b) POM with C2 chalk and POM with C3 chalk.

The presence of holes resulting from the cavitation certainly influences the ultimate properties of POM, facilitating its early fracture. During crystallization in occluded pocket of melt numerous bubbles usually appeared synchronously, i.e., within less than 0.04 s, at the spherulite-melt interface. It was already suggested[15,18] that the synchronous appearance of the group of bubbles could be a combined effect of the superposition of the negative pressure inside a weak spot and the acoustic wave produced by the primary cavitation event. Acoustic emission because of the cavitation during polymer crystallization was evidenced in the past by Galeski et al.[16] whereas Pease and Blinks[9] and recently Chow et al.[10] reported the pressure wave induced cavitation at crystallization front of low molecular weight substances.

The values of negative pressure causing cavitation are scattered for neat polymers, that is suggestive of nucleation controlled triggering of bubble formation and a different ability to nucleate the cavitation by various heterogeneous nuclei—the effect known well for low molecular weight liquids. The results obtained for POM based compositions with talc and chalk particles indicate clearly that the cavitation can be nucleated by foreign solid particles. In the case of POM with 5 wt % of C2 chalk only a single bubble appeared within a weak spot, the strength of the POM melt was greatly reduced and the scatter of cavitation threshold data was also eliminated. This result also points out that microscope glasses confining POM films did not play a significant role in the nucleation of cavitation.

The first cavitation event in POM with 5 wt % of modified C2 chalk did not trigger secondary cavitation events because it occurred at a low negative pressure. However, in POM with 1 wt % of the same chalk, the absolute value of negative pressure causing cavitation was higher, and several bubbles appeared synchronously inside the melt. Thus, the level of negative pressure relaxed by the primary cavitation event is crucial for triggering the cavitation in other sites.

The results obtained for neat POM and POM based compositions show clearly the influence of foreign solid particles on the cavitation of POM melt during crystallization. C2 chalk, modified with calcium stearate, decreased significantly the strength of POM melt and changed the way in which the cavitation occurred, whereas the unmodified chalk did not show any significant influence on cavitation. C3 chalk, modified with calcium stearate, but with particles smaller than those in C2 chalk, also nucleated the cavitation although less efficiently than C2 chalk. Whereas this observation underlines the significance of adhesion between a polymer and foreign solid particles present in the melt, there are also other important factors. A rough estimation reveals that in the composition of POM with 5 wt % of C2 chalk, a weak spot of initial surface area of 0.01 mm^2 should contain about 10^3–10^4 chalk particles, whereas only a single cavitation bubble was always nucleated by the most efficient nucleus. Since the first cavitation event relaxed the negative pressure, other nuclei possibly effective at the negative pressure of higher absolute value, remained inactive. The weakening of nucleation activity with the decrease of C2 chalk content in POM also indicates that only a fraction of chalk particles could act as the most effective nucleation sites for cavitation. Similarly as in low molecular weight liquids,[8] the heterogeneous nucleus of cavitation might be in the form of a solid particle with a crevice filled with gas. Thus, the topography of chalk particles surface might be crucial; good candidates for heterogeneous nuclei of cavitation are aggregates and agglomerates of chalk particles with air filled gaps between the particles. C3 chalk, with particles one order of magnitude smaller than those in C2 chalk was less efficient. If compositions with the same weight content of chalk are compared, the one with C3 chalk contains 10^3 times more particles than that with C2 chalk. Weakening of the effect with the decrease of particle size points out that not a number but a particle size as an important factor.

The nucleation of cavitation in the POM melt by talc used in this study was rather weak in contrast to the well known strong nucleation of POM crystallization.[28,29] The mineral used in this study is a mixture of minerals; thus whereas talc nucleates the crystallization, the nucleation of cavitation might be caused by one of the other two components: a chlorite or a dolomite.

Similarly as in iPP,[15] the influence of the initial size of the pocket of melt and the crystallization temperature on the buildup of negative pressure and cavitation were observed in neat POM. The ratio of circumference to the surface area is larger than smaller weak spots. This which enables easier relaxation of stresses by the deformation of surrounding spherulites. The increase of crystallization temperature reduces the spherulite growth rate, decreases the melt viscosity, leads to a coarser spherulitic structure and weaker bonding between crystalline, and amorphous phases. Thus, the displacement of a material within spherulites surrounding a melt pocket is easier which slows down the buildup of a negative pressure. The negative pressure reaches a considerable level when the crystallization within a melt pocket is advanced and the remaining melt volume is small; however, then the probability of the presence of a nucleus of cavitation is reduced.

The ultimate negative pressure causing cavitation of neat polymer melts was about −18 MPa, for both

the iPP[15] and POM. In comparison with tap water, which fractures even under positive pressure, slightly lower than the atmospheric pressure, polymers, even unpurified, exhibit high melt strength. This should be attributed to a difficulty of cavity formation in the polymer melt because of strong cohesion resulting from the entanglements of macromolecules.

References

1. Brennen, Ch. E. Cavitation and Bubble Dynamics; Oxford University Press: Oxford, 1995.
2. Fisher, J. C. J Appl Phys 1948, 19, 1062.
3. Fisher, J. C.; Hollomon, J. H.; Turnbull, D. J Appl Phys 1948, 19, 775.
4. Zheng, Q.; Durben, D. J.; Wolf, G. H.; Angell, C. A. Science 1991, 254, 829.
5. Berthelot, M. Ann Chim Phys 1850, 30, 232.
6. Henderson, S. J.; Speedy, R. J. J Phys E 1980, 13, 778.
7. Briggs, L. J. J Appl Phys 1950, 21, 721.
8. Harvey, E. N.; McElroy, W. D.; Whiteley, A. H. J Appl Phys 1947, 18, 162.
9. Pease, D. C.; Blinks, L. R. J Phys Chem 1947, 51, 556.
10. Chow, R.; Blindt, R.; Kamp, A.; Grocutt, P.; Chivers, R. Ind J Phys Part A 2003, 77, 315.
11. Galeski, A.; Piorkowska, E. J Polym Sci Polym Phys Ed 1983, 21, 1313.
12. Pawlak, A.; Galeski, A. J Polym Sci Part B: Polym Phys 1990, 28, 1813.
13. Pawlak, A.; Piorkowska, E. J Appl Polym Sci 1999, 74, 1380.
14. Thomann, R.; Wang, Ch.; Kressler, J.; Mulhaupt, R. Macromol Chem Phys 1996, 197, 1085.
15. Nowacki, R.; Kolasinska, J.; Piorkowska, E. J Appl Polym Sci 2001, 79, 2439.
16. Galeski, A.; Koenczol, L.; Piorkowska, E.; Baer, E. Nature 1987, 325, 40.
17. Galeski, A.; Piorkowska, E. J Polym Sci Polym Phys Ed 1983, 21, 1299.
18. Varga, J.; Ehrenstein, G. W. Polymer 1996, 37, 5959.
19. Pawlak, A.; Galeski, A. Macromolecules 2005, 38, 9688.
20. Galeski, A. Prog Polym Sci 2003, 28, 1643.
21. Piorkowska, E.; Nowacki, R. In Liquids Under Negative Pressure. NATO Science Series II. Mathematics, Physics and Chemistry; Imre, A. R.; Maris, H. J; Williams, P. R.; Eds.; Kluwer: Dordrecht, 2002; Vol. 84, p 137.
22. Monasse, B.; Haudin, J. M. Colloid Polym Sci 1985, 263, 822.
23. Monasse, B.; Haudin, J. M. Colloid Polym Sci 1988, 266, 679.
24. Mohanraj, J.; Bonner, M. J.; Barton, D. C.; Ward, I. M. Polymer 2006, 47, 5897.
25. Pelzbauer, Z.; Galeski, A. J Polym Sci Part C 1972, 38, 23.
26. Hoffman, J. D. Polymer 1983, 24, 3.
27. Karl, V. H.; Asmussen, F.; Ueberreiter, K. Makromol Chem 1977, 178, 2037.
28. Bayer, A. G. Brit. Pat. 1,133,490 (1968).
28. Bayer, A. G. Ger. Pat. 1,247,645 (1967).
29. Pelzbauer, Z.; Galeski, A. J Polym Sci Part C 1972, 38, 23.